# Comparison of Exact Solution With Eikonal Approximation for Elastic Heavy Ion Scattering

*Rajendra R. Dubey, Govind S. Khandelwal, Francis A. Cucinotta, and Khin Maung Maung*

# Comparison of Exact Solution With Eikonal Approximation for Elastic Heavy Ion Scattering

*Rajendra R. Dubey and Govind S. Khandelwal*
*Old Dominion University • Norfolk, Virginia*

*Francis A. Cucinotta*
*Langley Research Center • Hampton, Virginia*

*Khin Maung Maung*
*Hampton University • Hampton, Virginia*

This publication is available from the following sources:

## Summary

Numerical comparisons are made of an exact solution with the Eikonal approximation to the Lippman-Schwinger equation for an equivalent first-order optical potential for heavy ion scattering. The exact solution proceeds by using a partial-wave expansion of the Lippmann-Schwinger equation in momentum space. Calculations are made for the total and absorption cross sections for nucleus-nucleus scattering. The results are compared with solutions in the Eikonal approximation for the equivalent potential and with experimental data in the energy range from $25A$ to $1000A$ MeV. The percentage differences between the exact and Eikonal solutions are shown to be small above $200A$ MeV, but at lower energies, differences become large and corrections to the first-order optical model are required.

## Introduction

In high-energy nucleus-nucleus scattering, many nucleons can interact mutually and the structure of multiple scattering is richer than nucleon-nucleus scattering. A simple approach in nucleus-nucleus scattering is to consider the scattering in terms of each constituent of the projectile nucleus interacting with each constituent of the target nucleus. Other terms may contribute to the scattering, such as a projectile constituent interacting consecutively with two different constituents of target (i.e., double scattering). Similarly, contributions may come from three, four, and more successive scatterings. The formalism using this approach is called multiple scattering theory.

The nucleus-nucleus scattering processes are conveniently analyzed by employing an optical potential theory. Once the optical potential is determined, the original many-body scattering problem reduces to a two-body scattering problem. However, the price of reducing a many-body problem to a two-body situation is that the optical potential will be, in general, a complicated nonlocal, complex operator. Thus, for practical applications we shall require the approximation method to determine the optical potential.

An early generalization of the optical model ideas in nuclear physics to the study of alpha-decay of nuclei was made by Ostrofsky, Breit, and Johnson (ref. 1). Bethe (ref. 2) introduced the concept of an optical potential in order to describe low-energy nuclear reactions within the compound nucleus model. The description of high-energy nuclear collisions by means of the optical model formalism was initiated

by Fernbach, Serber, and Taylor (ref. 3), who first tried to describe elastic nucleon-nucleus scattering in terms of nucleon-nucleon collisions. They argued that at high energies, a nuclear collision should proceed by way of collisions with individual target nucleons by using known nucleon-nucleon cross sections. This multiple scattering analysis led to the conclusion that particles should move more or less freely through nuclear matter at high energies. The fact that the optical potential is complex is worth noticing. The imaginary part of the optical potential corresponds to the absorption of the incident beam by target nuclei, and the real part of the optical potential corresponds to the refraction of the beam without any disturbance to the target nuclei. Watson (ref. 4) and Kerman, McManus, and Thaler (KMT) (ref. 5) developed the formal theory of the scattering of high-energy nucleons by nuclei in terms of the nucleon-nucleon scattering amplitude.

A general multiple scattering theory for the scattering of two composite nuclei (neglecting three-body interactions) has been developed by Wilson (refs. 6 and 7). Calculations of the reaction and absorption for the heavy ion projectile was well developed by Wilson and Townsend (refs. 8 and 9) by using an Eikonal approximation to a first-order optical model. In the first-order optical model, the excitation of the projectile or target in intermediate states is neglected in elastic scattering. The Eikonal approximation is based on a forward scattering assumption, as well as considerations of the strength of the potential (refs. 6 and 10). A second-order solution to the Eikonal coupled-channels (ECC) model was developed by Cucinotta et al. (refs. 11 and 12) and was found to give improved accuracy over the first-order solutions in limited studies for several collision pairs and energies. The Eikonal approximation is computationally efficient because it requires only a few numerical integrations for implementation. In this report, neutron-nucleus, alpha-nucleus, and carbon-nucleus total and absorption cross sections are calculated by using the Lippmann-Schwinger equation. By comparing calculations with identical physical inputs that use the exact solution of the first-order optical model to the Eikonal approximate solutions, we provide an important validation of databases used in cosmic-ray studies. The Eikonal model is also unable to account for nuclear medium corrections, although such studies may be performed in the future by using momentum space methods. The treatment of medium corrections will be required if further improvements in nuclear databases are needed.

In the remainder of this paper, we present the formalism for the first-order optical model and partial-wave decomposition of the Lippman-Schwinger equation. In the following sections, we discuss the optical potential, the Eikonal model, model calculations describing physical inputs, and the comparison of exact and Eikonal solutions with experimental data.

## First-Order Optical Model and Partial-Wave Decomposition of Lippmann-Schwinger Equation

The total Hamiltonian $H$ satisfies the time-independent Schrodinger equation

$$H |\bar{\psi}\rangle = E|\bar{\psi}\rangle \tag{1}$$

where $E$ is the eigenvalue of operator $H$ and $|\bar{\psi}\rangle$ is the state vector. In case of nucleus-nucleus scattering, the total Hamiltonian is given by

$$H = H_P + H_T + V \tag{2}$$

where $V$ is the potential energy operator between projectile ($P$) and target ($T$) constituents. Here, $V$ is defined as

$$V = \sum_{j=1}^{A_P} \sum_{\alpha=1}^{A_T} v_{\alpha j} \tag{3}$$

where $j$ denotes the projectile, $\alpha$ denotes the target nucleus, $v_{\alpha j}$ is the interaction potential, and $A_P$ and $A_T$ denote the projectile and target mass numbers, respectively.

The transition operator for scattering the $\alpha$ constituent of the target with the $j$ constituent of the projectile is defined by the Lippmann-Schwinger equation (which is the integral form of the Schrödinger equation) as

$$\tau_{\alpha j} = v_{\alpha j} + v_{\alpha j} G_o \tau_{\alpha j} \tag{4}$$

(ref. 6) where $G_o$ is the Green's function given by

$$G_o = (E - H_P - H_T)^{-1} \tag{5}$$

The solution of the multiple scattering problem is generally intractable in the exact form. An approximate potential is developed by using the transition operator of equation (4) to replace the highly singular two-body potential. This is usually developed through an optical-potential formalism following the methods of Watson (ref. 4) or Kerman, McManus, and Thaler (ref. 5). Wilson and Townsend (refs. 6–8) have considered a first-order optical potential in the impulse approximation for nucleus-nucleus scattering which neglects the excitation of the projectile and target in the intermediate states for elastic scattering (coherent approximation). Here, the transition operator ($T$) obeys

$$T = U + U g_o T \tag{6}$$

where $g_o$ is the free two-body Green's function and the optical potential is given by

$$U = \sum_{\alpha j} t_{\alpha j} \tag{7}$$

where

$$t_{\alpha j} = \nu_{\alpha j} + \nu_{\alpha j} g_o t_{\alpha j} \tag{8}$$

An alternative derivation of a first-order optical potential for nucleus-nucleus scattering that considers antisymmetrization effects following the approach of reference 5 would lead to

$$U = \frac{A_P A_T - 1}{A_P A_T} \sum_{\alpha_j} t_{\alpha_j} \tag{9}$$

which is approximately the same as equation (7) for $A_P A_T \gg 1$.

To solve equation (6) we take the matrix element with respect to the projectile and target ground states. If $\mathbf{k}_1$ and $\mathbf{k}_2$ are wave vectors of two nucleons in the lab system, we define the relative wave vector as

$$\mathbf{k} = \frac{\mathbf{k}_1 - \mathbf{k}_2}{2} \tag{10}$$

If we take the half on-shell matrix element of $T$ in equation (6), we get

$$\langle \mathbf{k}' | \mathbf{T} | \mathbf{k} \rangle = \langle \mathbf{k}' | \mathbf{U} | \mathbf{k} \rangle + \int \frac{\langle \mathbf{k}' | \mathbf{U} | \mathbf{k}'' \rangle \langle \mathbf{k}'' | \mathbf{T} | \mathbf{k} \rangle d\mathbf{k}''}{E_k - E_{k''} + i\eta} \tag{11}$$

where $|\mathbf{k}\rangle$ is the on-shell wave vector. The $\mathbf{R}$ matrix satisfies

$$\langle \mathbf{k}' | \mathbf{R} | \mathbf{k} \rangle = \langle \mathbf{k}' | \mathbf{U} | \mathbf{k} \rangle + P \int \frac{\langle \mathbf{k}' | \mathbf{U} | \mathbf{k}'' \rangle \langle \mathbf{k}'' | \mathbf{R} | \mathbf{k} \rangle d\mathbf{k}''}{E_k - E_{k''}} \tag{12}$$

where $P$ denotes the principal value of the integral. The $\mathbf{R}$ matrix is related to the $\mathbf{T}$ matrix by the Heitler equation, which is given by

$$\mathbf{T} = \mathbf{R} - i\pi \mathbf{R}\, \delta(E - h_o)\, \mathbf{T} \tag{13}$$

after the partial-wave decomposition

$$R_l(k,k') = U_l(k,k') + \frac{2\mu}{\hbar^2} \int_0^\infty \frac{U_l(k',k'')\, R_l(k'',k)\, k''^2 dk''}{k^2 - k''^2} \tag{14}$$

where $\mu$ is the reduced mass. Thus, we have used the following expression for the partial wave decomposition:

$$\langle \mathbf{k}' | \mathbf{R} | \mathbf{k} \rangle = \sum_l \frac{2l+1}{4\pi}\, R_l(k',k)\, P_l(k',k) \tag{15}$$

The on-shell $T_l$ is related to the on-shell $R_l$ via the Heitler equation. Thus,

$$T_l = \frac{R_l(k,k)}{1 + \frac{i\pi\mu}{\hbar^2} k\, R_l(k,k)} \tag{16}$$

The nucleus-nucleus transition matrix $\mathbf{T}(q)$ and the scattering amplitude $f(q)$ for the nucleus-nucleus system are given by

$$\mathbf{T}(q) = \sum_{l=0}^\infty \frac{2l+1}{4\pi}\, T_l\, P_l(\cos\theta) \tag{17}$$

and

$$f(q) = -(2\pi)^2\, \frac{E_P\, E_T}{E_P + E_T}\, \mathbf{T}(q) \tag{18}$$

respectively, and the differential cross section is given by

$$\frac{d\sigma}{d\Omega} = |f(q)|^2 \tag{19}$$

Now, by integrating over a solid angle we obtain the total elastic cross section as

$$\sigma_{\text{el}} = \int |f(q)|^2 \, d\Omega \tag{20}$$

The total cross section is related to the forward scattering amplitude by the optical theorem as

$$\sigma_{\text{tot}} = \frac{4\pi}{k} \, \text{Im} \, f_{\text{el}}(\theta = 0) \tag{21}$$

where Im denotes the imaginary part. Thus, after $T_l$ is calculated from equations (14) and (16) by the matrix inversion method, the scattering amplitude can be obtained from equation (18) and the total cross section can be obtained from equation (21) by taking the imaginary part of the forward scattering amplitude. Now, the absorption cross section is simply obtained by

$$\sigma_r = \sigma_{\text{tot}} - \sigma_{\text{el}} \tag{22}$$

The expression for the scattering amplitude given by equation (18) requires an infinite number of partial waves for the **t** matrix to be calculated from equation (16), and usually truncating the sum to a finite number of partial waves is necessary. The results obtained are very reasonable at low energy. It is well known that as the projectile energy increases, the number of partial waves necessary also increases to make the sum in equation (17) divergent. It is also well known that for high partial waves and high energies, the Born approximation for the $l$th partial-wave component of $T_l$ is a good choice (i.e., $T_l \approx U_l$). We will utilize this fact to our advantage in order to make a correction for the contribution of higher partial waves. First, we rewrite equation (17) as

$$\mathbf{T}(q) = \sum_{l=0}^{l_{\text{max}}} \frac{2l+1}{4\pi} \, T_l P_l(\cos\theta) + \sum_{l_{\text{max}}+1}^{\infty} \frac{2l+1}{4\pi} \, T_l P_l(\cos\theta) \tag{23}$$

where $l_{\text{max}} + 1$ is the partial wave in which the Born approximation is good. This can be easily done by comparing $U_l$ and the calculated $T_l$ for each partial wave while solving equation (14). When making the Born approximation for the second term of equation (23), we obtain

$$\mathbf{T}(q) = \sum_{l=0}^{l_{\text{max}}} \frac{2l+1}{4\pi} \, T_l P_l(\cos\theta) + \sum_{l_{\text{max}}+1}^{\infty} \frac{2l+1}{4\pi} \, U_l P_l(\cos\theta)$$

$$+ \sum_{l=0}^{l_{\text{max}}} \frac{2l+1}{4\pi} \, U_l P_l(\cos\theta) - \sum_{l=0}^{l_{\text{max}}} \frac{2l+1}{4\pi} \, U_l P_l(\cos\theta) \tag{24}$$

in which we have added and subtracted a term in the last equation. Now, the second and third terms can combine to give us the three-dimensional $\mathbf{U}(q)$, because it is a sum of all partial waves for $U$. Therefore, we finally get

$$\mathbf{T}(q) = \sum_{l=0}^{l_{\text{max}}} \frac{2l+1}{4\pi} \, T_l P_l(\cos\theta) - \sum_{l=0}^{l_{\text{max}}} \frac{2l+1}{4\pi} \, U_l P_l(\cos\theta) + \mathbf{U}(q) \tag{25}$$

Equation (25) is the final result, which tells us that in order to obtain the contributions from the higher partial wave, we have to calculate $T_l$ only up to a certain $l_{\text{max}}$ at which the Born approximation becomes good. Then,

4

$\mathbf{T}(q)$ is obtained by summing $T_l$ to $l_{\max}$ and $\mathbf{U}(q)$ is added. At the end, the sum of $U_l$ up to $l_{\max}$ has to be subtracted to avoid double counting. The phase shift $\delta_l$ is given by

$$T_l = \frac{-\hbar^2}{\pi\mu} \frac{e^{2i\delta_l} - 1}{2ik} \tag{26}$$

The total elastic and absorption cross sections are defined (ref. 10) as

$$\sigma_{\mathrm{el}} = \frac{\pi}{k^2} \sum_{l=0}^{\infty} (2l+1)|\eta_l \ e^{2i \ \mathrm{Re} \ \delta_l} - 1|^2 \tag{27}$$

and

$$\sigma_r = \frac{\pi}{k^2} \sum_{l=0}^{\infty} (2l+1) \ (1 - \eta_l^2) \tag{28}$$

respectively, where Re denotes the real part and

$$\eta_l = e^{-2 \ \mathrm{Im} \ \delta_l} \tag{29}$$

Then, the total cross section is defined as

$$\sigma_{\mathrm{tot}} = \frac{2\pi}{k^2} \sum_{l=0}^{\infty} (2l+1)[1 - \eta_l \ \cos{(2 \ \mathrm{Re} \ \delta_l)}] \tag{30}$$

## Optical Potential

In the first-order optical model in the impulse approximation, the optical potential is the matrix element over target and projectile ground states of free two-body amplitude. Thus,

$$\langle f|\mathbf{U}|i\rangle = \frac{A_P A_T - 1}{A_P A_T} \ \langle 0_P 0_T \ \mathbf{k}'| \sum_{\alpha_j} t_{\alpha_j} |0_P 0_T \mathbf{k}\rangle \tag{31}$$

At this point we digress to discuss $t_{\alpha_j}$ and recall that the optical potential has a spin dependence that arises from the spin dependence of the $\mathbf{t}$ matrix. From symmetry principles, one can write the nonrelativistic $\mathbf{t}$ matrix for nucleon-nucleon scattering in terms of Pauli spin operators as

$$\begin{aligned}\mathbf{t} =&A + C \ (\boldsymbol{\sigma}_1 + \boldsymbol{\sigma}_2) \cdot \hat{n} + M \ \boldsymbol{\sigma}_1 \cdot \hat{m}\boldsymbol{\sigma}_2 \cdot \hat{m} + G \ \boldsymbol{\sigma}_1 \cdot \hat{n} \ \boldsymbol{\sigma}_2 \cdot \hat{n} + H\boldsymbol{\sigma}_1 \cdot \hat{l} \ \boldsymbol{\sigma}_2 \cdot \hat{l} \\ &+ D(\boldsymbol{\sigma}_1 \cdot \hat{m} \ \boldsymbol{\sigma}_2 \cdot \hat{l} + \boldsymbol{\sigma}_1 \cdot \hat{l} \ \boldsymbol{\sigma}_2 \cdot \hat{m}) \end{aligned} \tag{32}$$

(ref. 13) where $\boldsymbol{\sigma}$ is the Pauli spin operator and $(\hat{l}, \hat{m}, \hat{n})$ defines a right-hand coordinate system.

If we consider only spin-zero nuclei, and the spin projection of target and projectile nucleus is integrated out, the terms of $\mathbf{t}$ that are linear in the projectile and target nucleon spin are vanishing and leave only the first term $A$.

Thus, we get the optical potential for spin zero-spin-zero, nucleus-nucleus (NN) scattering as

$$\langle f|\mathbf{U}|i\rangle = \frac{A_P A_T - 1}{A_P A_T} \int dq \ A(q) \ F_P(q) \ G_T(q) \tag{33}$$

where $F_P$ is the projectile form factor and $G_T$ is the target form factor. Therefore, we write

$$A(q) = \frac{-\hbar^2}{(2\pi)^2\mu} \ f_{\mathrm{NN}}(q) \tag{34}$$

## Eikonal Model for Total and Absorption Cross Sections

The generalization of the Eikonal approximation to many-body scattering problems is given by Glauber (refs. 14 and 15), who applied it extensively to high-energy hadron-nucleus scattering. Wilson (ref. 6) has discussed the Eikonal approximation for the nucleus-nucleus optical model by using a coupled-channels formalism. In the Eikonal coupled channel (ECC) model (refs. 6 and 11), the matrix of scattering amplitudes for all possible projectile-target transitions is given by

$$\bar{\mathbf{f}}(\mathbf{q}) = \frac{-ik}{2\pi} \widehat{Z} \int d^2b \; e^{i\mathbf{q}\cdot\mathbf{b}} \left\{ e^{i\bar{\chi}(\mathbf{b})} - \bar{1} \right\} \tag{35}$$

where barred quantities represent matrices, $\mathbf{b}$ is an impact parameter vector, $\mathbf{q}$ is the momentum transfer vector, and $k$ is the projectile target relative wave number. In equation (35), $\widehat{Z}$ is an ordering operator for the $\widehat{Z}$-coordinate, which is necessary only when noncommuting two-body interactions are considered (ref. 11). The matrix elements of $\overline{\chi}(\mathbf{b})$ are written as

$$\langle 0_P 0_T | \overline{\chi}(\mathbf{b}) | 0_P 0_T \rangle = \frac{1}{2\pi k_{\mathrm{NN}}} \sum_{\alpha,j} \int d^2q \, e^{i\mathbf{q}\cdot\mathbf{b}} F_P(-q) \, G_T(q) \, f_{\mathrm{NN}}(q) \tag{36}$$

The first-order approximation to the elastic amplitude, which is obtained by neglecting all transitions between the ground and excited states and assuming that transitions between excited states are negligible, leads to

$$f^{(1)}(q) = \frac{-ik}{2\pi} \int d^2b \; e^{-i\mathbf{q}\cdot\mathbf{b}} \left\{ e^{i\chi} - 1 \right\} \tag{37}$$

(refs. 6 and 11) where

$$\chi(b) = \frac{A_P \, A_T}{2\pi \, k_{\mathrm{NN}}} \int d^2q \, e^{i\,\mathbf{q}\cdot\mathbf{b}} F_P(-q) \, G_T(q) \, f_{\mathrm{NN}}(q) \tag{38}$$

The total cross section found from the elastic amplitude by using the optical theorem from equations (21) and (37) is given as

$$\sigma_{\mathrm{tot}} = 4\pi \int\limits_0^\infty b \, db \, \{ 1 - \exp[(-\mathrm{Im}\,\chi)\cos(\mathrm{Re}\,\chi)] \} \tag{39}$$

The total absorption cross section that is found by subtracting the total elastic scattering cross section from equation (39) is

$$\sigma_r = 2\pi \int\limits_0^\infty b \, db \, \left\{ 1 - e^{-2\,\mathrm{Im}\,\chi} \right\} \tag{40}$$

## Model Calculations

The two-body scattering amplitude is parameterized as

$$f_{\mathrm{NN}}(q) = \frac{\sigma(\alpha + i)}{4\pi} k_{\mathrm{NN}} e^{-Bq^2/2} \tag{41}$$

where $\sigma$ is the nucleon-nucleon total cross section, $\alpha$ is the ratio of the real part to the imaginary part of the forward two-body amplitude, and $B$ is the slope parameter.

The one-body form factor is written in terms of the charge (CH) form factor as

$$F(q) = \frac{F_{\mathrm{CH}}(q)}{F_p(q)} \tag{42}$$

6

where $F_p(q)$ is the proton form factor. For light nuclei ($A < 16$), we use the harmonic well distribution

$$F_{CH} = (1 - sq^2)e^{-aq^2} \tag{43}$$

where the values for the parameters $s$ and $a$ are taken from reference 9. For medium and heavy mass nuclei ($A \geq 17$) where a Wood-Saxon density is appropriate,

$$\rho_{CH}^{(r)} = \frac{\rho_0(r)}{1 - \exp(\frac{r-R}{c})} \tag{44}$$

We use an exact Fourier transform from equation (44) to obtain the charge form factor found in the series solution given by

$$F_{CH}(q) = \frac{4\pi}{q} \rho_0(q) \; \phi(q) \tag{45}$$

(ref. 16) where

$$\phi(q) = \pi R c \left\{ \frac{-\cos(Rq)}{\sinh(\pi cq)} + \frac{\pi c}{R} \frac{\sin(Rq) \coth(\pi cq)}{\sinh(\pi cq)} - \frac{2c}{\pi R} \sum_{m=1}^{\infty} (-1)^m \frac{m \, c \, q \, e^{-mR/c}}{[(cq)^2 + m^2]^2} \right\} \tag{46}$$

The series in equation (46) converges rapidly, and the first three or four terms are accurate for most applications. Values for the parameters $c$ and $R$ are taken from reference 9.

## Discussion

By using the formalism described in previous sections, total and absorption cross sections for neutron, He, and C colliding with different target nuclei have been calculated in an energy range from $25A$ to $1000A$ MeV. By using the Lippmann-Schwinger calculation and the Eikonal model, theoretical predictions for total and absorption cross sections are compared in figures 1–6 with representative experimental data (refs. 18–22). All physical inputs (form factors and two-body amplitudes) are kept identical in the Lippmann-Schwinger and Eikonal model calculations. The agreement is excellent between the Lippmann-Schwinger calculation, the Eikonal model, and the experimental data at higher energy for total and absorption cross sections.

Calculations of the total cross sections for the nucleon-nucleus, helium-nucleus, and carbon-nucleus systems are shown in figures 1, 2, and 3, respectively. We observe from our calculations that at a lower energy, the percentage differences between the Eikonal model calculation and the exact calculation are higher when compared with those at higher energy. This is an indication that the Eikonal model prediction for scattering cross sections is fairly accurate at higher energies. The Eikonal model calculations are consistently lower than the exact calculations because of the forward scattering assumption of the Eikonal approximation. Although the scattering is dominated by forward angles at high energies,

some contribution from large-angle scattering is always present and is not represented by the Eikonal model. We also observe that both the Eikonal model and the exact calculations are well within the range of experimental data. At low energy, an improvement in the calculations will most likely occur by considering the corrections to the impulse approximation, correlation effects (refs. 17 and 23), or perhaps relativistic effects (ref. 24).

In figures 4, 5, and 6 we present comparisons of the partial-wave solution for the absorption cross section to the Eikonal model solution for the nucleon-nucleus, helium-nucleus, and carbon-nucleus systems, respectively. Experimental data are shown in these comparisons when available. The Eikonal model is seen to represent the exact solution quite well above projectile energies of $200A$ MeV, but below $200A$ MeV the differences are large. In some cases, the Eikonal model represents the experiment better than the exact solution, which is a definite indication that the first-order optical potential does not represent the complete physics at these lower energies because the Eikonal model is an approximation to the exact solution for the equivalent potential. Table 1 presents a comparison of the experimental data from reference 20 with the Eikonal and Lippmann-Schwinger calculations for carbon-nucleus absorption cross sections at an energy of $83A$ MeV. Although the calculations agree satisfactorily with experiment, further investigations of optical potential

theory, including nuclear medium effects, will be required for the theoretical evaluation of absorption cross sections with high precision at lower energies.

Table 1. Comparison of Experimental Data[a] With Calculations for Carbon-Nucleus Absorption Cross Sections

$[E_{\mathrm{lab}}/\mathrm{nucleon} = 83A\ \mathrm{MeV/nucleon}]$

| System | Values of $\sigma_r$, mb, for— | | |
|---|---|---|---|
|  | Experimental | Lippmann-Schwinger | Eikonal |
| $^{12}\mathrm{C} + {}^{12}\mathrm{C}$ | $960 \pm 30$ | 874 | 849 |
| $^{12}\mathrm{C} + {}^{27}\mathrm{Al}$ | $1400 \pm 40$ | 1419 | 1477 |
| $^{12}\mathrm{C} + {}^{40}\mathrm{Ca}$ | $1550 \pm 60$ | 1750 | 1737 |
| $^{12}\mathrm{C} + {}^{56}\mathrm{Fe}$ | $1810 \pm 100$ | 2123 | 1997 |

[a]For the carbon nucleus, the experimental data are taken from Kox et al. (ref. 20).

Figure 7 shows the number of partial waves required to calculate the total, absorption, and elastic cross sections at energies of $100A$ and $1000A$ MeV for nucleon-carbon and carbon-carbon systems. We observe from the calculations that if we increase the energy of the projectile, we will need more and more partial waves for the calculation of cross sections. Figure 8 shows the total and absorption cross sections as the function of the slope parameter at energies of $100A$ and $1000A$ MeV for the n-$^{16}$O system. We observe from our calculations that because the total and absorption cross sections saturate at large values of the slope parameter, a limiting value is reached.

## Concluding Remarks

The exact calculation of the Lippmann-Schwinger equation for a first-order optical potential was considered for light and heavy nuclei-induced reactions in an energy range from $25A$ to $1000A$ MeV. Comparisons with Eikonal approximate solutions and experimental data for target nuclei most important for space radiation studies were quite favorable and provided validation for earlier calculations used in cosmic-ray transport codes. The percentage differences at high energy between the Eikonal calculation and the exact calculation were small compared with those at low energy. Further improvements in the calculations will most likely occur by considering corrections to the impulse approximation and correlation effects, rather than to the first-order optical potential model employed in this paper.

NASA Langley Research Center
Hampton, VA 23681-0001
January 6, 1995

## References

1. Ostrofsky, M.; Breit, G.; and Johnson, D. P.: The Excitation Function of Lithium Under Proton Bombardment. *Phys. Rev.*, vol. 49, Jan. 1, 1936, pp. 22–34.

2. Bethe, H. A.: A Continuum Theory of the Compound Nucleus. *Phys. Rev.*, vol 57, June 15, 1940, pp. 1125–1144.

3. Fernbach, S.; Serber, R.; and Taylor, T. B.: The Scattering of High Energy Neutrons by Nuclei. *Phys. Rev.*, vol. 75, no. 9, May 1, 1949, pp. 1352–1355.

4. Watson, Kenneth M.: Multiple Scattering and the Many-Body Problem—Applications to Photomeson Production in Complex Nuclei. *Phys. Rev.*, vol. 89, no. 3, Feb. 1953, pp. 575–578.

5. Kerman, A. K.; McManus, H.; and Thaler, R. M.: The Scattering of Fast Nucleons From Nuclei. *Ann. Phys.* (N.Y.), vol. 8, no. 4, Dec. 1959, pp. 551–635.

6. Wilson, John W.: Composite Particle Reaction Theory. Ph.D. Diss., College of William and Mary, June 1975.

7. Wilson, J. W.: Multiple Scattering of Heavy Ions, Glauber Theory, and Optical Model. *Phys. Lett.*, vol. B52, no. 2, Sept. 1974, pp. 149–152.

8. Wilson, J. W.; and Townsend, L. W.: An Optical Model for Composite Nuclear Scattering. *Canadian J. Phys.*, vol. 59, no. 11, 1981, pp. 1569–1576.

9. Townsend, Lawrence W.; and Wilson, John W.: *Tables of Nuclear Cross Sections for Galactic Cosmic Rays—Absorption Cross Sections.* NASA RP-1134, 1985.

10. Joachain, Charles J.: *Quantum Collision Theory.* Elsevier Publ. Co., 1975.

11. Cucinotta, Francis A.: Theory of Alpha-Nucleus Collisions at High Energies. Ph.D. Thesis, Old Dominion Univ., 1988.

12. Cucinotta, Francis A.; Khandelwal, Govind S.; Maung, Khin M.; Townsend, Lawrence W.; and Wilson, John W.: *Eikonal Solutions to Optical Model Coupled-Channel Equations.* NASA TP-2830, 1988.

13. Johnson, Mikkel B.; and Picklesimer, Alan, ed.: *Relativistic Dynamics and Quark-Nuclear Physics.* John Wiley & Sons, 1986.

14. Glauber, Roy J.: Potential Scattering at High Energies. *Phys. Rev.*, vol. 91, Sept. 1953, p. 459.

15. Glauber, R. J.: Cross Sections in Deuterium at High Energies. *Phys. Rev.*, vol. 100, no. 1, Oct. 1, 1955, pp. 242–248.

16. Maung, Khin Maung; Deutchman, P. A.; and Royalty, W. D.: Integrals Involving the Three-Parameter Fermi Function. *Canadian J. Phys.*, vol. 67, nos. 2 & 3, Feb.–Mar. 1989, pp. 95–99.

17. Cucinotta, F. A.; Khandelwal, G. S.; Townsend, L. W.; and Wilson, J. W.: Correlations in $\alpha$–$\alpha$ Scattering and Semi-Classical Optical Models. *Phys. Lett.*, vol. B223, no. 2, June 8, 1989, pp. 127–132.

18. Franz, J.; Grotz, H. P.; Lehmann, L.; Rossle, E.; Schmitt, H.; and Schmitt, L.: Total Neutron-Nucleus Cross Sections at Intermediate Energies. *Nucl. Phys.*, vol. A490, 1988, pp. 667–688.

19. Shiver, L.; and Kanai, T.: Energy Loss, Range and Fluence Distributions, Total Reaction and Projectile Fragmentation Cross Sections in Protron-Nucleus and Nucleus-Nucleus Interactions. NIRS-M-87, HIMAC-002, National Institute of Radiological Sciences, July 1992.

20. Kox, S.; Gamp, A.; Cherkaoui, R.; Cole, A. J.; Longequeue, N.; Menet, J.; Perrin, C.; and Viano, J. B.: Direct Measurements of Heavy-Ion Total Reaction Cross Sections at 30 and 83 MeV/Nucleon. *Nucl. Phys.*, vol. A420, no. 1, May 21, 1984, pp. 162–172.

21. Bauhoff, W.: Tables of Reaction and Total Cross Sections for Proton-Nucleus Scattering Below 1 GeV. *At. Data & Nucl. Data Tables*, vol. 35, no. 3, Nov. 1986, pp. 429–448.

22. Sourkes, A. M.; Houdayer, A.; Van Oers, W. T. H.; Carlson, R. F.; and Brown, Ronald E.: Total Reaction Cross Section for Protons on $^3$He and $^4$He Between 18 and 48 MeV. *Phys. Rev. C*, vol. 13, no. 2, Feb. 1976, pp. 451–460.

23. Cucinotta, Francis A.; Townsend, Lawrence W.; and Wilson, John W.: *Target Correlation Effects on Neutron-Nucleus Total, Absorption, and Abrasion Cross Sections.* NASA TM-4314, 1991.

24. Maung, Khin Maung; and Gross, Franz: Covariant Multiple Scattering Series for Elastic Projectile-Targe Scattering. *Phys. Rev. C*, vol. 42, no. 4, Oct. 1990, pp. 1681–1693.

(a)  n-$^4$He scattering.

(b)  n-$^{12}$C scattering.

(c)  n-$^{16}$O scattering.

(d)  n-$^{27}$Al scattering.

(e)  n-$^{64}$Cu scattering.

(f)  n-$^{208}$Pb scattering.
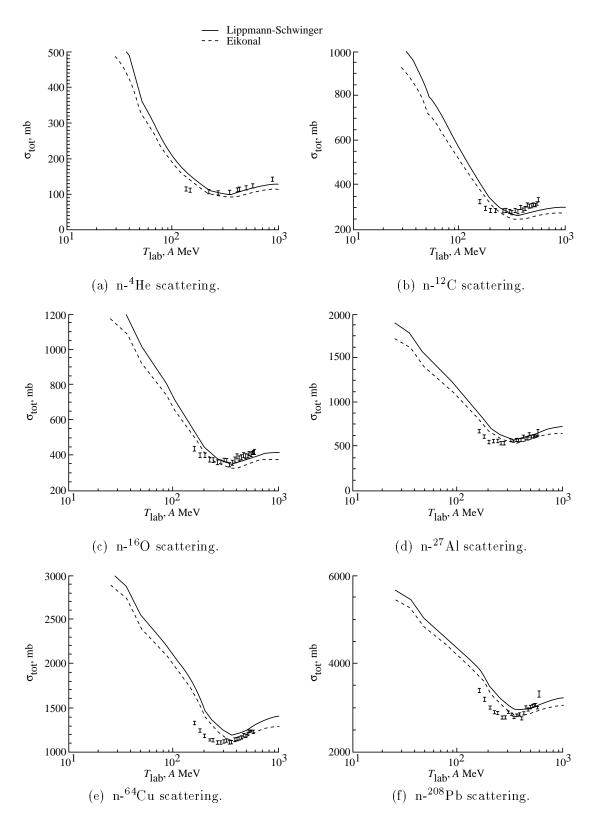
Figure 1. Comparison of total cross section calculation using Eikonal approximation with exact solution using equation (30) for nucleon-nucleus system in energy range from $25A$ to $1000A$ MeV. Available experimental data are shown by error bars.
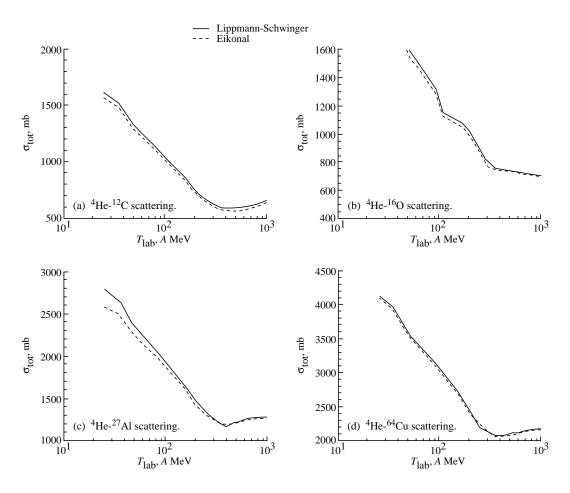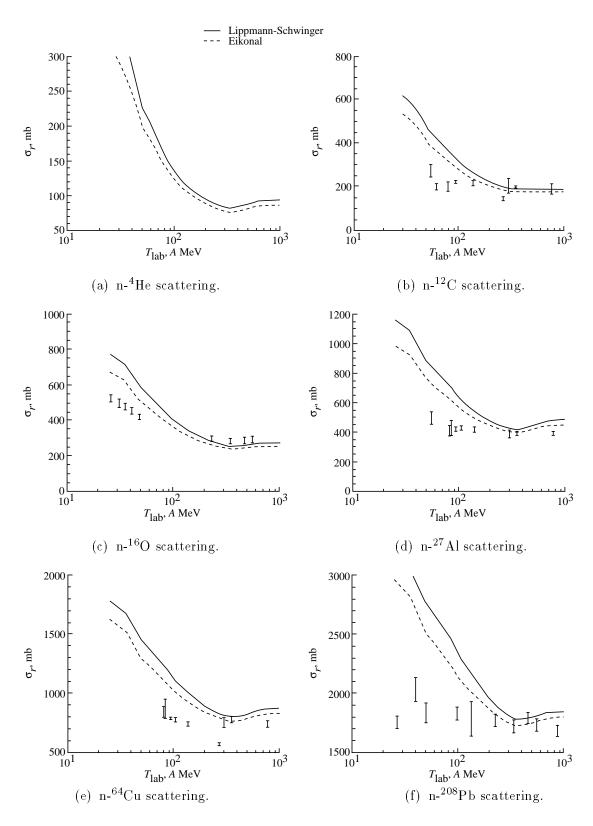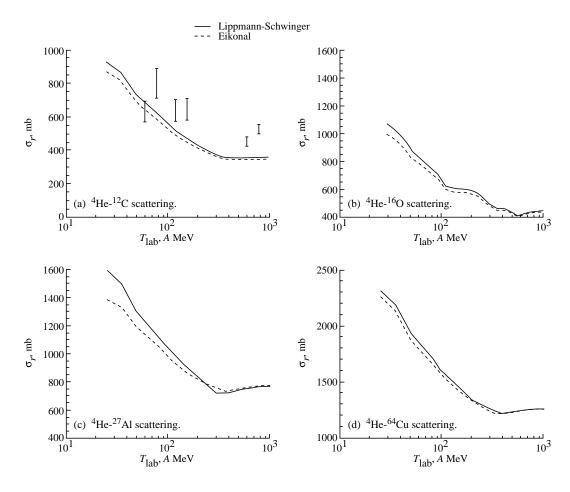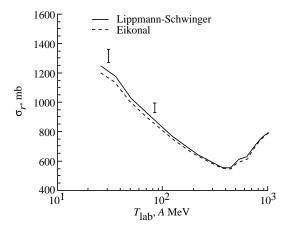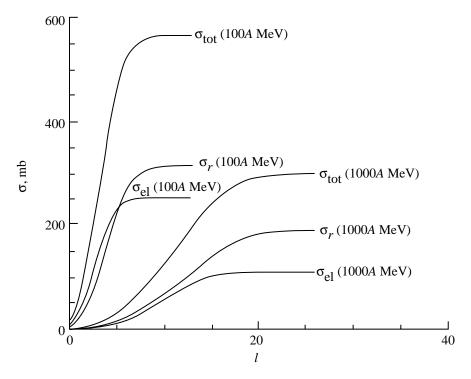
Figure 2. Comparison of total cross section calculation using Eikonal approximation with exact solution using equation (30) for helium-nucleus system in energy range from $25A$ to $1000A$ MeV.
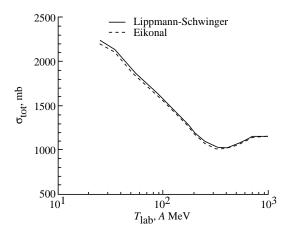


Figure 3. Comparison of total cross section calculation using Eikonal approximation with exact solution using equation (30) for carbon-nucleus system in energy range from $25A$ to $1000A$ MeV.

(a) n-$^4$He scattering.

(b) n-$^{12}$C scattering.

(c) n-$^{16}$O scattering.

(d) n-$^{27}$Al scattering.

(e) n-$^{64}$Cu scattering.

(f) n-$^{208}$Pb scattering.

Figure 4. Comparison of absorption cross section calculation using Eikonal approximation with exact solution using equation (29) for nucleon-nucleus system in energy range from $25A$ to $1000A$ MeV. Available experimental data are shown by error bars.

Figure 5. Comparison of absorption cross section calculation using Eikonal approximation with exact solution using equation (29) for helium-nucleus system in energy range from $25A$ to $1000A$ MeV. Available experimental data are shown by error bars.



Figure 6. Comparison of absorption cross section calculation using Eikonal approximation with exact solution using equation (29) for carbon-nucleus system in energy range from $25A$ to $1000A$ MeV. Available experimental data are shown by error bars.

(a) $100A$ and $1000A$ MeV for n-$^{12}$C system.



(b) $100A$ MeV for $^{12}$C-$^{12}$C system.
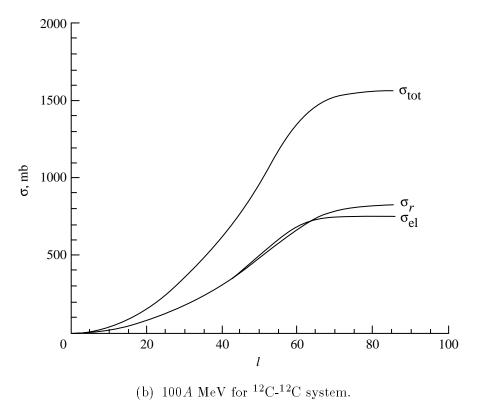
Figure 7. Comparison of total, absorption, and elastic cross sections as a function of number of partial waves.

(a)  $100A$ MeV for n-$^{16}$O system.



(b)  $1000A$ MeV for n-$^{16}$O system.
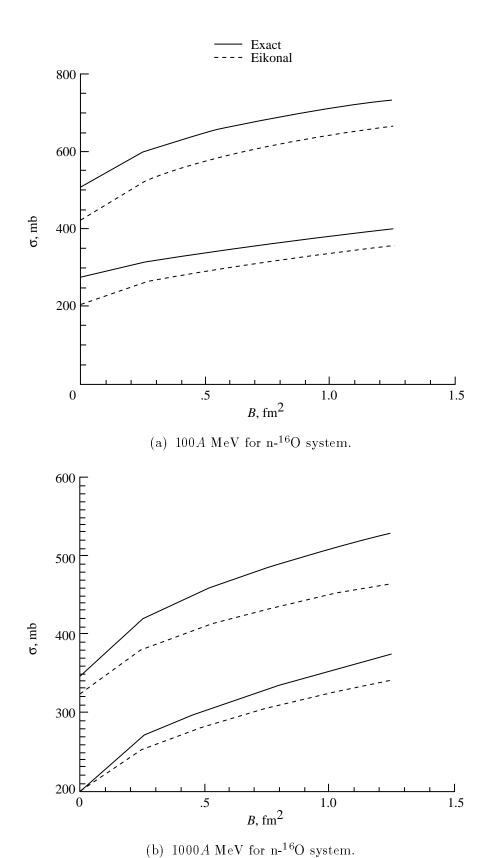
Figure 8. Comparison of total and absorption cross sections for exact and Eikonal calculations as a function of slope parameter.

# REPORT DOCUMENTATION PAGE

Public reporting burden for this collection of information is estimated to average 1 hour per response, including the time for reviewing instructions, searching existing data sources, gathering and maintaining the data needed, and completing and reviewing the collection of information. Send comments regarding this burden estimate or any other aspect of this collection of information, including suggestions for reducing this burden, to Washington Headquarters Services, Directorate for Information Operations and Reports, 1215 Jefferson Davis Highway, Suite 1204, Arlington, VA 22202-4302, and to the Office of Management and Budget, Paperwork Reduction Project (0704-0188), Washington, DC 20503.

| 1. AGENCY USE ONLY(Leave blank) | 2. REPORT DATE | 3. REPORT TYPE AND DATES COVERED |
|---|---|---|
| | February 1995 | Technical Paper |

**4. TITLE AND SUBTITLE**
Comparison of Exact Solution With Eikonal Approximation for Elastic Heavy Ion Scattering

**5. FUNDING NUMBERS**
WU 199-45-16-11

**6. AUTHOR(S)**
Rajendra R. Dubey, Govind S. Khandelwal, Francis A. Cucinotta, and Khin Maung Maung

**7. PERFORMING ORGANIZATION NAME(S) AND ADDRESS(ES)**
NASA Langley Research Center
Hampton, VA 23681-0001

**8. PERFORMING ORGANIZATION REPORT NUMBER**
L-17428

**9. SPONSORING/MONITORING AGENCY NAME(S) AND ADDRESS(ES)**
National Aeronautics and Space Administration
Washington, DC 20546-0001

**10. SPONSORING/MONITORING AGENCY REPORT NUMBER**
NASA TP-3498

**11. SUPPLEMENTARY NOTES**
Dubey and Khandelwal: Old Dominion University, Norfolk, VA; Cucinotta: Langley Research Center, Hampton, VA; Maung: Hampton University, Hampton, VA.

**12a. DISTRIBUTION/AVAILABILITY STATEMENT**

Unclassified–Unlimited
Subject Category 73
Availability: NASA CASI, (301) 621-0390

**12b. DISTRIBUTION CODE**

**13. ABSTRACT** (Maximum 200 words)
A first-order optical potential is used to calculate the total and absorption cross sections for nucleus-nucleus scattering. The differential cross section is calculated by using a partial-wave expansion of the Lippmann-Schwinger equation in momentum space. The results are compared with solutions in the Eikonal approximation for the equivalent potential and with experimental data in the energy range from $25A$ to $1000A$ MeV.

**14. SUBJECT TERMS**
Heavy ions; Total and absorption cross sections; Galactic cosmic rays

**15. NUMBER OF PAGES**
16

**16. PRICE CODE**
A03

| 17. SECURITY CLASSIFICATION OF REPORT | 18. SECURITY CLASSIFICATION OF THIS PAGE | 19. SECURITY CLASSIFICATION OF ABSTRACT | 20. LIMITATION OF ABSTRACT |
|---|---|---|---|
| Unclassified | Unclassified | Unclassified | |

NSN 7540-01-280-5500

Standard Form 298(Rev. 2-89)
Prescribed by ANSI Std. Z39-18
298-102